ZEOLITE-CATALYZED RING-SHIFT ISOMERIZATION OF *sym*-OCTAHYDROPHENANTHRENE INTO *sym*-OCTAHYDROANTHRACENE. EXPERIMENTAL RESULTS AND CALCULATED EQUILIBRIUM COMPOSITIONS

Wei-Chuan Lai, Chunshan Song*, Adri van Duin[§] and J. W. de Leeuw[§]
Fuel Science Program, 209 Academic Projects Building,
The Pennsylvania State University, University Park, Pennsylvania 16802, U.S.A
[§]Division of Marine Biogeochemistry, Netherlands Institute of Sea Research (NIOZ),
P.O. Box 59, 1790 AB Den Burg, The Netherlands

Keywords: Zeolites, isomerization, octahydrophenanthrene, octahydroanthracene

INTRODUCTION

Phenanthrene and its derivatives are abundant in coal-derived liquids from coal carbonization, pyrolysis, and liquefaction; however, they are used in industries only to a limited extent despite of considerable efforts [Song and Schobert, 1993]. On the other hand, their isomers, anthracene and its derivatives such as *sym*-octahydroanthracene (*sym*-OHA), are more useful materials for industrial applications. Anthracene and its derivatives may be used as the starting materials for the manufacturing of anthraquinone (an effective pulping accelerator), pyromellitic dianhydride (PMDA, the monomer for polyimides such as Du Pont's Kapton), and dyestuffs [Song and Schobert, 1993, 1995]. Thus, it is desirable to convert phenanthrenes to anthracenes.

There has been much research on the catalytic hydroprocessing of phenanthrene under high H_2 pressures and at temperatures generally in excess of 623 K [Nakatsuji et al., 1978; Haynes et al., 1983; Salim and Bell, 1984; Lee and Satterfield, 1993; Girgis and Gates, 1994; Landau et al., 1994; Korre et al., 1995]. However, relatively little information about the ring-shift isomerization of phenanthrenes into anthracenes at lower temperatures is available. It has been shown in our earlier exploratory work that some chemically modified mordenites and Y-zeolites may selectively promote the transformation of *sym*-octahydrophenanthrene (*sym*-OHP) into *sym*-OHA [Song and Moffatt, 1993, 1994]. Cook and Colgrove (1994) reported the acid catalyzed isomerization of phenanthrene, anthracene, and *sym*-OHA under FCC conditions (755 K). The objective of this work is to clarify the effects of reaction conditions and catalyst properties on the catalytic isomerization of *sym*-OHP into *sym*-OHA. In addition, the Molecular Mechanics (MM3) [Allinger et al., 1990] calculations were performed to find the equilibrium compositions of *sym*-OHP and *sym*-OHA, and to establish the upper limit of the catalytic conversion. We wish to establish activity and selectivity data that could point to an inexpensive way of making anthracene derivatives from phenanthrene derivatives.

EXPERIMENTAL

The *sym*-OHA and *sym*-OHP chemicals were obtained from Aldrich Chemical Company and TCI America, respectively, and were used as received. Their purities were analyzed in our laboratory using gas chromatography (GC) and gas chromatography-mass spectrometry (GC-MS). The catalysts used in the catalytic isomerization reactions include: two hydrogen mordenites (HML8 and HM30A) and two noble metal loaded mordenites (Pt/HM30A and Pd/HM30A). Pt/HM30A and Pd/HM30A were prepared by incipient wetness impregnation method; i.e., the salt of platinum and palladium were dispersed into the mordenites by incipient wetness impregnation of corresponding aqueous H_2PtCl_6 or H_2PdCl_4 dissolved in hydrochloric acid. The noble metal loading on the support was kept at nominally 6 wt%. The metal-loaded catalysts were calcined in air at 723 K for 2 h after being dried in vacuum oven. The details of the preparation and properties of the catalysts are described elsewhere [Song and Moffatt, 1994; Schmitz et al., 1994].

Catalytic isomerization reactions were carried out in 28-mL horizontal type stainless steel tubing bomb reactors, which were charged with 0.6 mmole of *sym*-OHP or *sym*-OHA (0.112 g), 1 ml of 1,3,5-trimethylbenzene solvent, and 0.2 g of catalyst, at 473–573 K for 0.15-12 h under an initial pressure of 0.79 MPa UHP N_2 or H_2. The uniformity of concentration and temperature inside the reactor was obtained by agitating the reactor vertically at 240 cycles/min. After the reaction, the gas products were collected in a gas bag, and the liquid products were recovered by washing with acetone. The recovered catalyst was stored in a vial for thermogravimetric analysis performed later. The gaseous products were quantitatively analyzed using a Perkin-Elmer Autosystem GC equipped with two detectors, a thermal conductivity detector (TCD) and a flame ionization detector (FID). The liquid products were analyzed on an HP 5890II GC coupled with an HP 5971A Mass Selective Detector (MSD) and quantified by a Perkin-Elmer GC 8500 equipped with an FID. More details for the analytical procedures may be found elsewhere [Song et al., 1994].

RESULTS AND DISCUSSION

Calculated equilibrium compositions from MM3. The equilibrium compositions of *sym*-OHP and *sym*-OHA at three temperatures were calculated to establish the theoretical upper limit of the catalytic conversion. The procedures are as follows. Calculations on the various conformers present in an equilibrium mixture containing only *sym*-OHA and *sym*-OHP were first performed. In order to obtain the raw geometries for the molecules and to find the different conformers present, the DELPHI-molecular mechanics program was used with the MM3 force field. The obtained minimized geometries were used as starting points for the MM3 program, using the MM3 force field (both the 1992 versions). Only slight differences were found between the optimized DELPHI- and MM3-geometries. Five and six different conformers were found for *sym*-OHA and *sym*-OHP,

respectively, as shown in Table 1. Table 1 also shows the calculated heats of formation and entropies for the different conformations of *sym*-OHA and *sym*-OHP at 298 K. The literature value of the heat of formation of *sym*-OHA is -8.89 kcal/mol [Pedley et al., 1986]. The good agreement between the literature value (-8.89 kcal/mol) and the calculated one (-9.17 kcal/mol, in Table 1) indicates that the MM3 force field should be applicable to problems like these. From these data, the Gibbs free energy of *sym*-OHA and *sym*-OHP at 298 K could be obtained. In similar fashion, the Gibbs free energies of these compounds at 473, 523, and 573 K may be calculated by correcting the heats of formation and entropies in Table 1 for temperatures. From these free energies, the equilibrium composition of the *sym*-OHA/*sym*-OHP mixture was calculated. It should be noticed that one may get different MM3 calculation results from using different estimated thermodynamic parameters of *sym*-OHA and *sym*-OHP. It was found that the error in the MM3 calculations using current parameters for such kind of mixture compositions is about 10%. The calculated mixture compositions will be presented later and compared with experimental data following the presentation of experimental results.

Effectiveness of HML8. HML8 was studied more extensively than other catalysts in this work, because it was found to be the best among several zeolitic catalysts in our previous work at 523 K for 2 h [Song and Moffatt, 1993, 1994]. Table 2 presents the results of *sym*-OHP isomerization over HML8 with *sym*-OHP as the starting material at three different temperatures (473, 523, and 573 K) under N_2 environment. The purity analysis results of the starting material was also presented in Table 2. It can be seen that the as-received reactant contains about 91% of *sym*-OHP, 2.9% of *sym*-OHA, 5.5% in total of various hydrogenated phenanthrenes (*asym*-OHP, 9,10-DHP, 1,2,3,4,4a,10a-HHP, and 1,2,3,4-THP), and 0.6% of other impurities. The purity analysis is important, because without this information it is possible that impurities are mistaken as products. The reactivities of 9,10-DHP and 1,2,3,4,4a,10a-HHP will be briefly discussed first. 9,10-DHP does not react to a great extent except under severe conditions, e.g., 573 K for 1 h; on the other hand, 1,2,3,4,4a,10a-HHP reacts quickly even at a lower temperature, 473 K. The main reaction of 9,10-DHP, which accounts for about 2.7% of the starting reactant, was believed to be dehydrogenation to phenanthrene under current reaction conditions. The supporting evidence is from the fact that the sum of 9,10-DHP and phenanthrene was relatively constant (about 2.8) for most of the reaction conditions. Other researchers also suggested the hydrogenation of 9,10-DHP to 1,2,3,4-THP [Lemberton and Guisnet, 1984] and *asym*-OHP [Nakatsuji et al., 1978]; however, these hydrogenation reactions are less likely under the current reaction conditions judging from the deficiency of hydrogen and the overall product distribution of 1,2,3,4-THP and *asym*-OHP. To verify this, experiments need to be performed with 9,10-DHP as the sole reactant. For 1,2,3,4,4a,10a-HHP, the main reactions were believed to include dehydrogenation to 1,2,3,4-THP, and ring-contraction isomerization and ring-opening cracking.

The major reaction of interest in this work is the isomerization of *sym*-OHP to *sym*-OHA; Table 2 shows that HML8 was an effective catalyst for this reaction because it could afford over 90% selectivity with reasonable conversion (about 50%). In order to approach equilibrium conditions, relatively long residence times have been employed, e.g., 12 h at 473 K, 4 h at 523 K, and 1 h at 573 K. From Table 2, the reactions seemed to have reached the asymptotic equilibrium after 12 h at 473 K, 2 h at 523 K, and 0.25 h at 573 K. In other words, the yield of *sym*-OHA reached its maximum at those reaction conditions, and longer reaction times at 523 K and 573 K only served to decrease the *sym*-OHA yield because of enhanced competitive side-reactions or secondary reactions such as ring-opening cracking and subsequent dealkylation (to form mainly alkyltetralins), conventional ring-contraction isomerization, and dehydrogenation. The selectivity towards *sym*-OHA suffered severely when the reaction temperature was increased to 573 K, when side-reactions became significant.

Table 3 compares the pseudo-equilibrium yields from MM3 calculations and experimental results at three temperatures. There exists discrepancy between the calculated data and the experimental results. The MM3 calculations indicate that the reaction temperature has a moderate effect on the equilibrium ratio of *sym*-OHA to *sym*-OHP. For example, the ratio changes from 2.56 to 1.95 when the temperature is increased from 473 K to 573 K. However, the experiments show that although the reaction temperature affects the reaction rate and selectivity, the equilibrium ratio is not sensitive to the reaction temperature. For example, the equilibrium ratios are all close to 1.3 for the temperature range studied. Table 3 shows that the pseudo-equilibrium yields of *sym*-OHA from experiments are considerably lower than the calculated equilibrium yield from MM3 method. There might be some explanations for the discrepancy. The calculation assumes that *sym*-OHP and *sym*-OHA are the only reacting species in the reaction system. However in the real experimental system since there are other reactants as well as by-products, the actual equilibrium state now depends on more simultaneous chemical reactions. For the current reaction system, at higher temperatures, e.g., 523 K and 573 K, there are significant side reactions as can be seen from the smaller *sym*-OHA selectivity or the decreasing sum of *sym*-OHP and *sym*-OHA. Other simultaneous reactions might include the reactions due to the solvent used (1,3,5-trimethylbenzene) as well. Since many reactions are involved, the composition is a resultant of all the operative reactions and is determined by the thermodynamic equilibrium for the total system. In short, the presence of such simultaneous reactions have shifted the equilibrium state of *sym*-OHA and *sym*-OHP.

Some experiments using purc *sym*-OHA (rather than *sym*-OHP) as starting material were also performed to check the reversibility of the ring-shift isomerization and to confirm the experimentally obtained pseudo-equilibrium composition (Table 3). The results of *sym*-OHA isomerization over HML8 with *sym*-OHA as the starting material at three temperatures under N_2 environment are given

in Table 4. The results demonstrate the reversibility of the ring-shift isomerization. Besides, it was shown again that HML8 was quite selective for the ring-shift isomerization except under severe conditions. From Table 4, the reactions seemed to have reached pseudo-equilibrium after 4 h at 473 K, 0.5 h at 523 K, and 0.15 h at 573 K judging from the fact that the yield of *sym*-OHP reached its maximum at those reaction conditions. The pseudo-equilibrium compositions of sym-OHA and sym-OHP and their ratios reported in Table 4 are very close to those reported earlier (see Tables 2 and 3); for example, the equilibrium ratio is not sensitive to the reaction temperature and is close to 1.3. From the data in Tables 2-4, on the basis of reaction rate alone, it appears desirable to operate the reaction at a high temperature level such as 573 K. However, an examination of the reaction selectivity reveals that the selectivity towards *sym*-OHA drops rapidly at 573 K due to significant side-reactions. Taking both rate and selectivity into consideration, it seems that 523 K for 0.5 h might be the desirable condition for the *sym*-OHP isomerization over HML8.

Effectiveness of HM30A. HM30A was used to examine the possible effect of dealumination on the ring-shift isomerization in comparison to HML8. The SiO_2/Al_2O_3 molar ratios of HML8 and HM30A are 17 and 35, respectively. Table 5 presents the results of *sym*-OHP isomerization over HM30A with *sym*-OHP as the starting material at two temperatures (473 and 523 K) under N_2. Tables 2 and 5 suggest that both catalysts reacted comparably near the pseudo-equilibrium condition at 473 K for 12 h; this could be seen from the similar conversion level, selectivity, and *sym*-OHA to *sym*-OHP ratio. However, at 523 K, they behaved slightly different. The H-mordenites with relatively larger SiO_2/Al_2O_3 ratio, i.e., HM30A, seem to exhibit higher activity for *sym*-OHP conversion but lower selectivity towards *sym*-OHA plus THA. The comparison of selectivity could be seen at similar conversion level, 51.9%, where the selectivity is 91.9% and 83.5% for HML8 and HM30A, respectively. In short, HM30A shows promising results at 473 K in terms of both activity and selectivity, but is not as selective as HML8 at 523 K. More experiments with additional catalysts will be needed to clarify the effect of dealumination on the ring-shift isomerization.

Effectiveness of Pt/HM30A and Pd/HM30A. The motivation of using these two noble metal loaded mordenites on the ring-shift isomerization comes from the promising activity and selectivity results of HM30A at 473 K as well as our study on conformational isomerization of *cis*-decalin using the same two catalysts [Lai and Song, 1995]. It was found that Pt- and Pd-loaded mordenites are very effective catalysts under H_2 atmosphere for the conformational isomerization of *cis*-decalin even at 473 K. Because of their high activity and selectivity on the isomerization of naphthalene derivatives, Pt/HM30A and Pd/HM30A were also used in this study. Table 6 presents the results of isomerization over these two catalysts with *sym*-OHP or *sym*-OHA as the starting material at 473 K under 0.79 MPa of H_2 or N_2.

The effect of noble metals can be seen by comparing the results of HM30A (PS42, in Table 5) and those of Pt- and Pd-loaded HM30A (PS47 and PS48, respectively, see Table 6). Mordenites loaded with noble metal exhibits much higher activity but lower selectivity towards hydrogenated anthracenes. The activity for *sym*-OHP conversion is: Pd/HM30A > Pt/HM30A > HM30A. The lower selectivity towards *sym*-OHA for both Pd/HM30A and Pt/HM30A is due to the significant dehydrogenation reactions to form THA and THP or even phenanthrene under N_2 environments. The results are not beyond expectation because both Pt and Pd are well known active metals for dehydrogenation and hydrogenation. Hydrogenation was not apparent because of the H_2 deficient environment, since reactions were performed under N_2. The dehydrogenation activity drops in the order Pd > Pt.

As can be seen from Table 6, changing the gas environment from N_2 to H_2 significantly affects the final product distribution because the dehydrogenation under N_2 was replaced with hydrogenation under H_2. Figure 1 presents the temporal plots of major products from *sym*-OHP isomerization using Pt/HM30A and Pd/HM30A at 473 K under excess H_2 (8 mmole). Figure 1 provides information about the reaction pathways. For example, for the catalyst Pt/HM30A, it can be seen that *sym*-OHA was the primary product; its yield reached a maximum at 0.3 h and then decreased due to enhanced hydrogenation. On the other hand, PHA and PHP appeared to be the secondary products resulting from hydrogenation of OHA or OHP. Table 6 shows that for Pt/HM30A after 0.3-h reaction time, the ratio of sym-OHA to sym-OHP approached a constant value of 1.28, which was very close to the pseudo-equilibrium mole ratio determined from the study of HML8 and HM30A. All these results suggest that *sym*-OHA formation be the major primary reaction and hydrogenation of OHP and OHA did not occur until *sym*-OHA and *sym*-OHP reached pseudo-equilibrium. In addition, it was demonstrated that Pt/HM30A shows promising activity and selectivity at 473 K under H_2. Optimal products may be reached in a short period of time, e.g., 0.15-0.3 h. Longer reaction time under H_2 environment beyond the pseudo-equilibrium stage is not beneficial to the production of *sym*-OHA, due to pronounced hydrogenation to form deeper hydrogenation products such as perhydrophenanthrene and perhydroanthracene .

The other noble metal catalyst, Pd/HM30A, showed slightly different results. Pd again shows higher activity but lower selectivity towards hydrogenated anthracenes. Its superior hydrogenation ability might have changed the reaction pathways. For example, instead of being a secondary product only, PHP might as well be a primary product too. The hydrogenation and isomerization reactions might have proceeded in parallel instead of in series for Pd/HM30A under H_2 environment. The supporting evidence is that the ratio of *sym*-OHA to *sym*-OHP did not approach the pseudo-equilibrium mole ratio until very late in the reaction when sym-OHP was almost completely consumed. The results seem to suggest that such strong ability of dehydrogenation and

hydrogenation might make Pd a less favorable catalyst for the ring-shift isomerization of *sym*-OHP. The results of *sym*-OHA isomerization over Pt/HM30A and Pd/HM30A with *sym*-OHA as the starting material under H_2 environment, are also given in Table 6. The results demonstrate the reversibility of the ring-shift isomerization and the important role of deeper hydrogenation.

SUMMARY

The MM3 calculations were performed to find the equilibrium compositions of *sym*-OHP and *sym*-OHA and were compared to experimental results using four catalysts including HML8, HM30A, Pt/HM30A, and Pd/HM30A. The MM3 calculations showed a moderate effect of the reaction temperature on the equilibrium ratio of *sym*-OHA to *sym*-OHP. However, the experiments showed that although the reaction temperature affected the reaction rate and selectivity, the equilibrium ratio was not sensitive to the reaction temperature. The presence of simultaneous side reactions was believed to have shifted the equilibrium state. The rate and selectivity of the isomerization reactions depended on both the metal and support type of the catalysts, but the equilibrium ratio was not sensitive to the catalysts used and was close to a constant value of 1.3. The activity for *sym*-OHP conversion is: Pd/HM30A > Pt/HM30A > HML8 ≈ HM38. Longer reaction time beyond the pseudo-equilibrium stage was not beneficial to the production of *sym*-OHA, especially for Pd/HM30A and Pt/HM30A due to the pronounced hydrogenation or dehydrogenation. Pt/HM30A showed promising activity and selectivity at 473 K under H_2 with optimal reaction time of 0.15-0.3 h. The desirable condition for HML8 was 523 K for 0.5 h. HM30A showed promising results at 473 K, but was not as selective as HML8 at 523 K. Too strong an ability of dehydrogenation and hydrogenation might make Pd/HM30A a less favorable catalyst for the ring-shift isomerization of *sym*-OHP.

ACKNOWLEDGMENTS

We are grateful to Dr. T. Golden and Dr. V. Schillinger for providing the mordenites samples, and to Dr. A. Schmitz of PSU for preparing the noble metal catalysts. C.S. would like to thank Prof. H. H. Schobert and Prof. P. B. Weisz for their encouragement.

REFERENCES

Allinger, N. L.; Li, F.; Yan, L.; Tai, J. C. *J. Computational Chem.* **1990**, *11*, 868-895.
Cook, B. R.; Colgrove, S. G. *Prepr.-Am. Chem. Soc., Div. Pet. Chem.* **1994**, *39* (3), 372-378.
Girgis, M. J.; Gates, B. C. *Ind. Eng. Chem. Res.* **1994**, *33*, 1098-1106.
Haynes, H. W. Jr.; Parcher, J. F.; Helmer, N. E. *Ind. Eng. Chem. Process Des. Dev.* **1983**, *22*, 401-409.
Korre, S. C.; Klein, M. T.; Quann, R. J. *Ind. Eng. Chem. Res.* **1995**, *34*, 101-117.
Lai, W.-C.; Song, C. *Prepr.-Am. Chem. Soc., Div. Fuel Chem.* **1995**, *40*, in press.
Landau, R. N.; Korré, S. C.; Neurock, M.; Klein, M. T. In *Catalytic Hydroprocessing of Petroleum and Distillates.* M. C. Oballa and S. S. Shih, Eds., Marcel Dekker, Inc.: New York, **1994**, pp421-432.
Lee, C. M.; Satterfield, C. N. *Energy & Fuel* **1993**, *7*, 978-980.
Lemberton, J.-L.; Guisnet, M. *Appl. Catal.* **1984**, *13*, 181-192.
Nakatsuji, Y.; Kubo, T.; Nomura, M.; Kikkawa, S. *Bull. Chem. Soc. Jpn.* **1978**, *51*, 618-624.
Pedley, J. B.; Naylor, R. D.; Kirby, S. B. *Thermochemical Data of Organic Compounds.* **1986**, Chapman and Hall: London.
Salim, S. S.; Bell, A. T. *Fuel* **1984**, *63*, 469-476.
Schmitz, A. D.; Bowers, G.; Song, C. In *Advanced Thermally Stable Jet Fuels.* Technical Report, U.S. Department of Energy, DE-FG22-92PC92104-TPR-9, October **1994**, H. H. Schobert et al., Eds., pp37-42.
Song, C.; Moffatt, K. *Prepr.-Am. Chem. Soc., Div. Pet. Chem.* **1993**, *38* (4), 779-783.
Song, C.; Schobert, H. H. *Fuel Processing Technology* **1993**, *34*, 157-196.
Song, C.; Lai, W.-C.; Schobert, H. H. *Ind. Eng. Chem. Res.* **1994**, *33*, 534-547.
Song, C.; Moffatt, K. *Microporous Materials* **1994**, *2*, 459-466.
Song, C.; Schobert, H. H. *Prepr.-Am. Chem. Soc., Div. Fuel Chem.* **1995**, *40* (2), 249-259.

Table 1. The calculated heats of formation and entropies at 298 K

Conformation	ΔH_f (kcal/mole)	S (cal/mol-K)
sym-octahydroanthracene		
double chair (symmetric)	-9.17	105.54
double chair (asymmetric)	-9.17	105.54
boat-chair	-6.08	109.27
double boat (symmetric)	-3.00	107.48
double boat (asymmetric)	-3.03	107.47
sym-octahydrophenanthrene		
double chair (symmetric)	-7.98	106.33
double chair (asymmetric)	-7.57	106.89
boat-chair I	-5.05	108.78
boat-chair II	-4.83	108.76
double boat (symmetric)	-1.72	108.82
double boat (asymmetric)	-1.62	108.71

Table 2. *sym*-OHP isomerization over HML8 with *sym*-OHP as the starting material

Expt. no.	Temp. (K)	Time (h)	Products (wt% of feed)									X[c] (%)	Sel.[d] (%)	Ratio *sym*-OHA / *sym*-OHP
			sym-OHA	THA[a]	*sym*-OHP	*asym*-OHP[a]	9,10-DHP[a]	HHP[a]	THP[a]	Phen.[a]	Others[b]			
		0.0[e]	2.90		91.04	0.32	2.67	1.74	0.77	0.07	0.50			0.03
PS6	473	0.50	14.70	0.11	77.99	0.35	2.78	0.43	1.40	0.15	2.10	13.1	91.2	0.19
PS8	473	1.00	28.10	0.21	64.38	0.34	2.59	0.52	1.20	0.20	2.45	26.7	95.3	0.44
PS9	473	2.00	42.30	0.26	50.35	0.36	2.57	0.22	1.16	0.20	2.58	40.7	97.5	0.84
PS14	473	4.00	49.64	0.33	42.25	0.35	2.60	0.04	1.21	0.17	3.41	48.8	96.5	1.17
PS15	473	6.00	51.44	0.45	40.20	0.33	2.54	0.04	1.29	0.16	3.55	50.8	96.4	1.28
PS41	473	12.0	52.15	0.42	40.07	0.35	2.62	0.04	1.24	0.17	2.94	51.0	97.4	1.30
PS10	523	0.25	35.90	0.48	55.62	0.36	2.53	0.51	1.21	0.20	3.18	35.4	94.5	0.65
PS1	523	0.50	48.76	1.00	40.70	0.30	2.53	0.12	1.67	0.33	4.59	50.3	93.1	1.20
PS3	523	2.00	49.32	1.30	39.11	0.22	2.23	0.03	1.65	0.49	5.65	51.9	91.9	1.26
PS18	523	4.00	47.74	1.56	38.42	0.13	1.95		1.88	0.75	7.57	52.6	88.2	1.24
PS13	573	0.15	44.96	1.21	41.20	0.20	2.20	0.12	2.03	0.60	7.48	49.8	86.8	1.09
PS7	573	0.25	45.50	1.95	36.58	0.10	1.50	0.27	2.26	0.80	11.04	54.5	81.8	1.24
PS4	573	0.50	42.67	2.13	35.64	0.15	1.75	0.12	3.70	1.12	12.72	55.4	75.6	1.20
PS5	573	1.00	33.62	3.20	27.19	0.10	0.80	0.12	3.98	1.53	29.46	63.9	53.1	1.24

[a] THA = 1,2,3,4-tetrahydroanthracene; *asym*-OHP = 1,2,3,4,4a,9,10,10a-octahydrophenanthrene; 9,10-DHP = 9,10-dihydrophenanthrene; HHP = 1,2,3,4,4a,10a-hexahydrophenanthrene; THP = 1,2,3,4-tetrahydrophenanthrene; Phen. = phenanthrene.

[b] Others include products of ring-contraction isomerization and ring-opening cracking and subsequent dealkylation.

[c] X = conversion of *sym*-OHP (weight % of feed).

[d] Selectivity to *sym*-OHA plus THA, defined as the percentage of *sym*-OHP conversion.

[e] This row presents the purity of as-received *sym*-OHP.

Table 3. Pseudo-equilibrium composition of the *sym*-OHA/*sym*-OHP mixture

Temperature (K)	MM3 calculation		Experimental data[a]	
	OHA : OHP	Ratio	OHA : OHP[b]	Ratio
473	71.9% : 28.1%	2.56	52.2% : 40.1%	1.30
523	68.7% : 31.3%	2.19	49.3% : 39.1%	1.26
573	66.1% : 33.9%	1.95	45.5% : 36.6%	1.24

[a] Data from Table 2: 12 h at 473 K, 2 h at 523 K, and 0.25 h at 573 K.

[b] Other products make up the remainder.

Table 4. *sym*-OHA isomerization over HML8 with *sym*-OHA as the starting material

Expt. no.	Temp. (K)	Time (h)	Products (wt% of feed)						X[a] (%)	Sel.[b] (%)	Sel.[c] (%)	Ratio *sym*-OHA / *sym*-OHP
			sym-OHA	THA	*sym*-OHP	HHP	THP	Others				
PS27	473	1.00	61.44	0.23	35.52	0.18	0.08	2.54	38.6	92.1	92.8	1.73
PS28	473	4.00	55.07	0.40	41.22	0.14	0.10	3.07	44.9	91.7	92.3	1.34
PS33	473	8.00	55.42	0.39	40.56	0.16	0.09	3.38	44.6	91.0	91.5	1.37
PS25	523	0.25	56.18	0.67	37.95	0.25	0.20	4.75	43.8	86.6	87.6	1.48
PS26	523	0.50	53.36	0.76	40.69	0.27	0.30	4.62	46.6	87.2	88.5	1.31
PS32	523	2.00	51.38	1.04	39.91	0.19	0.57	6.91	48.6	82.1	83.6	1.29
PS29	573	0.15	50.91	1.26	39.15	0.23	0.92	7.53	49.1	79.8	82.1	1.30
PS30	573	0.25	45.97	1.67	36.39	0.18	1.57	14.22	54.0	67.4	70.6	1.26
PS31	573	0.50	40.65	2.28	32.36	0.16	2.52	22.03	59.4	54.5	59.0	1.26

[a] X = conversion of *sym*-OHA (weight % of feed, *sym*-OHA).

[b] Selectivity to *sym*-OHP, defined as the percentage of *sym*-OHA conversion.

[c] Selectivity to *sym*-OHP plus HHP and THP, defined as the percentage of *sym*-OHA conversion.

Table 5. *sym*-OHP isomerization over HM30A with *sym*-OHP as the starting material

Expt. no.	Catalyst type	Temp. (K)	Time (h)	Products (wt% of feed)									X[a] (%)	Sel.[b] (%)	Ratio *sym*-OHA / *sym*-OHP
				sym-OHA	THA	*sym*-OHP	*asym*-OHP	9,10-DHP	HHP	THP	Phen.	Others			
			0.00[c]	2.90		91.04	0.32	2.67	1.74	0.77	0.07	0.50			0.03
PS42	HM30A	473	12.00	52.57	0.64	39.03	0.30	2.39	0.14	1.40		3.53	52.0	96.7	1.35
PS16	HM30A	523	0.50	44.47	1.72	39.19	0.21	1.55	0.14	2.34	1.05	9.33	51.9	83.5	1.13
PS17	HM30A	523	1.00	42.87	2.06	35.90	0.12	1.20	0.11	2.54	1.29	13.91	55.1	76.2	1.19

Table 6. Ring-shift isomerization over noble metal loaded mordenites with *sym*-OHP or *sym*-OHA as the starting material at 473 K under 0.79 MPa of H_2 or N_2

Catalyst		Pt/HM30A						Pd/HM30A				
Time (h)	0.00[f]	0.30	0.15	0.30	1.00	2.00	2.00	0.30	0.15	0.30	2.00	2.00
Starting reactant		OHP	OHP	OHP	OHP	OHP	OHA	OHP	OHP	OHP	OHP	OHA
0.79-MPa N_2 or H_2		N_2	H_2	H_2	H_2	H_2	H_2	N_2	H_2	H_2	H_2	H_2
Expt. no.		PS47	PS45	PS43	PS36	PS39	PS38	PS48	PS46	PS44	PS37	PS40
Products (wt% of feed)												
sym-OHA	2.90	42.52	47.82	48.07	40.62	34.76	37.21	38.10	30.17	26.53	8.01	4.03
THA		7.77				0.20	0.05	9.00				
PHA[a]			2.57	3.70	9.94	12.63	12.06		10.00	16.72	33.77	40.11
sym-OHP	91.04	33.07	40.16	38.28	31.72	27.13	29.44	29.99	36.17	24.80	6.47	3.21
asym-OHP	0.32	1.14	2.62	3.53	3.67	3.65	3.61	1.95	4.23	3.47	1.55	0.82
9,10-DHP	2.67	0.71	0.01		0.03	0.13	0.14	1.47	0.01			
HHP	1.74	0.02	0.02	0.06	0.06	0.03		0.02	0.02	0.08		
THP	0.77	10.45			0.12	0.91	0.36	12.66				
Phenanthrene	0.06	3.35						5.20				
PHP[a]		0.08	5.25	5.06	11.53	15.12	13.24	0.07	16.94	25.34	45.85	47.40
Others	0.50	0.89	1.55	1.30	2.31	5.44	3.89	1.54	2.46	3.06	4.35	4.43
X (%)[b]		58.0	50.9	52.8	59.3	63.9	62.8	61.1	54.9	66.2	84.6	96.0
Selectivity[c] (%)		81.7	93.3	92.6	80.3	69.9		72.4	67.9	60.9	46.0	
Selectivity[d] (%)							46.9					3.3
Selectivity[e] (%)							74.5					53.6
sym-OHA/*sym*-OHP	0.03	1.29	1.19	1.26	1.28	1.28	1.26	1.27	0.83	1.07	1.24	1.26

[a] PHA = perhydroanthracene; PHP = perhydrophenanthrene.
[b] X = conversion of *sym*-OHP or *sym*-OHA (weight % of feed).
[c] Selectivity to *sym*-OHA plus THA and PHA, defined as the percentage of *sym*-OHP conversion.
[d] Selectivity to *sym*-OHP, defined as the percentage of *sym*-OHA conversion.
[e] Selectivity to hydrogenated phenanthrenes, defined as the percentage of *sym*-OHA conversion.
[f] This column presents the purity of as-received *sym*-OHP.

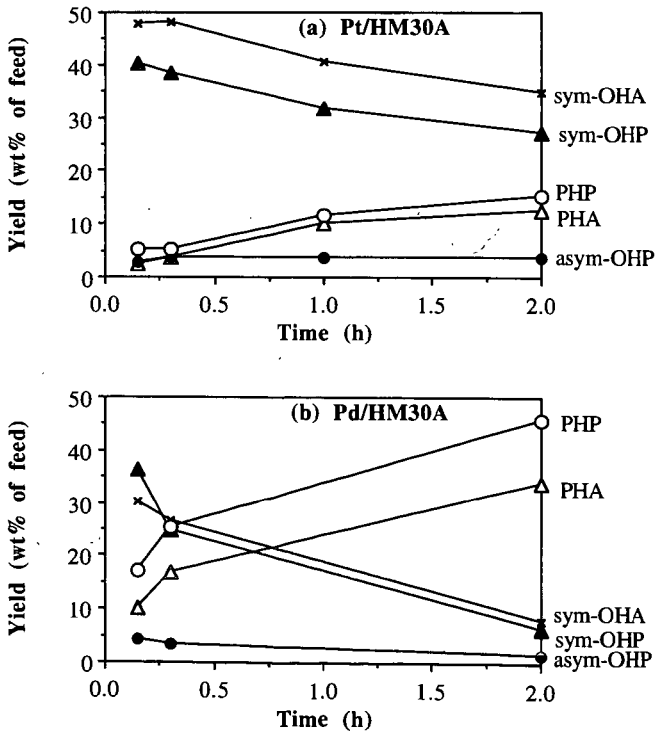

Figure 1. Temporal plots of major products from *sym*-OHP isomerization at 473 K under H_2.